

Numerical Renormalization Group Study of non-Fermi-liquid State on Dilute Uranium Systems

Yukihiro SHIMIZU*, Osamu SAKAI¹ and Shunya SUZUKI¹

Department of Applied Physics, Tohoku University, Sendai 980-8579

¹*Department of Physics, Tohoku University, Sendai 980-8578*

(Received May 10, 2018)

We investigate the non-Fermi-liquid (NFL) behavior of the impurity Anderson model (IAM) with non-Kramers doublet ground state of the f^2 configuration under the tetragonal crystalline electric field (CEF). The low energy spectrum is explained by a combination of the NFL and the local-Fermi-liquid parts which are independent with each other. The NFL part of the spectrum has the same form to that of two-channel-Kondo model (TCKM). We have a parameter range that the IAM shows the $-\ln T$ divergence of the magnetic susceptibility together with the positive magneto resistance. We point out a possibility that the anomalous properties of $U_x\text{Th}_{1-x}\text{Ru}_2\text{Si}_2$ including the decreasing resistivity with decreasing temperature can be explained by the NFL scenario of the TCKM type. We also investigate an effect of the lowering of the crystal symmetry. It breaks the NFL behavior at around the temperature, $\delta/10$, where δ is the orthorhombic CEF splitting. The NFL behavior is still expected above the temperature, $\delta/10$.

KEYWORDS: non-Fermi-liquid, impurity Anderson model, dilute Uranium compound, magnetization, magneto resistance, numerical renormalization group

§1. Introduction

The material, $U_x\text{Th}_{1-x}\text{Ru}_2\text{Si}_2$, seems to show the non-Fermi-liquid (NFL) behavior even in the dilute uranium limit.^{1,2,3)} Its magnetic susceptibility and γ -coefficient of the specific heat show the $-\ln T$ divergence at the low temperatures. At the same time the electrical resistivity decreases with decreasing temperature. Particular interests have been aroused in the NFL behavior driven by the single site effect.⁴⁾ This material has the tetragonal type structure, and the valence of the uranium ion is expected to be mainly, U^{4+} ($5f^2$). The crystalline electric field (CEF) ground state is also expected to be the non-Kramers doublet state from the measurement of the magnetization.

Many theoretical studies have been done for the NFL behavior of the dilute uranium compounds. Cox has pointed out the possibility that the electronic state of ion with f^2 configuration in a specific

* E-mail: yshzmz@snow.apph.tohoku.ac.jp

situation can be mapped on the $S=1/2$ -two-channel Kondo model ($S=1/2$ -TCKM),^{5,6)} which is known to show the NFL behavior.^{7,8,9,10)} The required situation is that the lowest CEF state of the f^2 configuration is the non-Kramers doublet state, and two kinds of conduction electrons, both of which have doubly degenerate time reversal pair, can hybridize with the f state. However, there are two remained problems in the application of the $S=1/2$ -TCKM to the NFL behavior of $U_x\text{Th}_{1-x}\text{Ru}_2\text{Si}_2$: First, the $S=1/2$ -TCKM can not explain the decrease of the resistivity with decreasing temperature. Usually opposite temperature dependence is expected when the coefficient of the $-\ln T$ term of the magnetic susceptibility is sizable.^{11,12)} Secondly, the mapping is done assuming very restricted situation. It is not clear whether the NFL state is stable or not when the realistic situation of the CEF states is taken into account. For the first problem we have modified the TCKM, and have proposed the extended two-channel Anderson model (ETCAM) that shows similar behaviors of the resistivity and the magnetic susceptibility to those of the experiment.^{13,14)} However, applicability of the ETCAM to the uranium problem is not obvious at present, because the intimate one-to-one mapping of electronic state has not been verified. In this paper, we check whether the anomalous properties of $U_x\text{Th}_{1-x}\text{Ru}_2\text{Si}_2$ can be explained or not based on a more realistic model.

For the second problem Koga and Shiba have studied the stability of the NFL state by taking into account the first excited state of the f^2 configuration.^{15,16,17)} They applied the numerical renormalization group (NRG) method, and has shown that the NFL state is still stable, if the CEF splitting is large. In previous paper, we have also studied the stability of the NFL state based directly on the impurity Anderson model (IAM),¹⁸⁾ because preceding studies have been done applying the Schrieffer-Wolff transformation by assuming the strong correlation limit. It has been shown that the ground state property can change to the NFL state from the usual Kondo type singlet state when the intensity of the hybridization is gradually weakened, even though all CEF states are taken into account, and the valence is apart from f^2 . But details of the low energy properties of the NFL state have not been clarified.

The first purpose of this paper is to analyze the low energy spectrum of the IAM given by the NRG method in detail.¹⁹⁾ We examine the model that the single electron orbitals split into three doublets under the tetragonal CEF. The CEF ground state is the non-Kramers doublet of f^2 configuration. In §3 we show that the low energy spectrum is explained by a combination of two components which are given by the NFL and the local-Fermi-liquid (LFL) fixed point Hamiltonians, and which are independent with each other. The NFL part of the low energy spectrum has the same form to that of the TCKM. The second purpose is to consider whether the anomalous behavior in $U_x\text{Th}_{1-x}\text{Ru}_2\text{Si}_2$ is explained from the IAM or not. In §4 and 5 we show that the large $-\ln T$ term of the magnetic susceptibility can be expected together with the positive magneto resistance at very low temperature, when the hybridization is not so weak. The positive magneto resistance indicates

that the temperature dependence of the resistivity decreases with decreasing temperature. The third purpose is to study the effect of the releasing process of the residual entropy which is inherent of the $S=1/2$ -TCKM. In §6 we examine the NFL behavior in the magnetization by breaking the NFL state with lowering the crystal symmetry.

§2. Model

We consider the following IAM under tetragonal CEF,

$$\mathcal{H} = \mathcal{H}_f + \mathcal{H}_{cf} + \mathcal{H}_c, \quad (2.1)$$

$$\begin{aligned} \mathcal{H}_f = & \sum_{\Gamma\gamma} \varepsilon(\Gamma) n_{f\Gamma\gamma} + \frac{U}{2} \sum_{(\Gamma\gamma) \neq (\Gamma'\gamma')} n_{f\Gamma\gamma} n_{f\Gamma'\gamma'} \\ & - \frac{I}{49} \sum_{\{\Gamma\gamma\}} \left[j_{\Gamma\gamma\Gamma'\gamma'} j_{\Gamma''\gamma''\Gamma'''\gamma'''} f_{\Gamma\gamma}^\dagger f_{\Gamma'\gamma'} f_{\Gamma''\gamma''}^\dagger f_{\Gamma'''\gamma'''} \right. \\ & \left. - \frac{35n_f}{4} \right], \end{aligned} \quad (2.2)$$

$$\mathcal{H}_{cf} = \sum_k \sum_{\Gamma\gamma} \left(V f_{\Gamma\gamma}^\dagger c_{k\Gamma\gamma} + \text{h.c.} \right), \quad (2.3)$$

$$\mathcal{H}_c = \sum_k \sum_{\Gamma\gamma} \varepsilon_k c_{k\Gamma\gamma}^\dagger c_{k\Gamma\gamma}, \quad (2.4)$$

where $f_{\Gamma\gamma}$ ($c_{k\Gamma\gamma}$) is the annihilation operator of f-electron with the γ -th component of Γ -irreducible representation (conduction electron with wave number k), and $\varepsilon(\Gamma)$, U and I denote the single f-electron energy, Coulomb and exchange interaction constants, respectively. For simplicity we assume the large spin-orbit interaction of f-electron, so only the $j = 5/2$ orbitals are considered. The orbitals split into a quartet, Γ_8 , and a doublet, $|f^1\Gamma_7^{(2)}, \pm\rangle = \pm\sqrt{1/6}|\pm 5/2\rangle \mp\sqrt{5/6}|\mp 3/2\rangle$ under the cubic CEF where m in $|m\rangle$ of the right hand side of the equation is the magnetic quantum number of j .²⁰⁾ The quartet splits into two doublets again, $|f^1\Gamma_7^{(1)}, \pm\rangle = \pm\sqrt{5/6}|\pm 5/2\rangle \pm\sqrt{1/6}|\mp 3/2\rangle$ and $|f^1\Gamma_6, \pm\rangle = |\pm 1/2\rangle$ under the tetragonal CEF. The Coulomb and the exchange interactions are assumed to be the j - j coupling type. Usually, the multiplet structure of U ion is approximated by the L - S coupling scheme. So the present j - j coupling scheme seems to be not applicable to U ion at first glance. However, we note the ground multiplets have same total angular momentum for both coupling schemes. We expect qualitative features of the low energy states within the ground multiplet will be not so changed. It is assumed the f-electron hybridizes with the conduction electron which has the same component of the irreducible representation. The quantities, V and ε_k denote the hybridization matrix and the band energy, respectively. It is also assumed the band is extending in energy from $-D$ to D with constant hybridization matrix, $\Gamma = \pi V^2/2D$. The energy unit and the origin of the energy are chosen as $D = 1$ and the Fermi level, respectively.

We rewrite the Hamiltonian into a form to suite the NRG calculation. First the conduction band

is discretized by the logarithmic mesh to give good sampling to states near the Fermi energy.²¹⁾ Next the Hamiltonian is transformed into an expression given by the shell orbits,

$$\mathcal{H} = \lim_{L \rightarrow \infty} \mathcal{H}_L, \quad (2.5)$$

$$\mathcal{H}_L = \mathcal{H}_f + \sum_{\Gamma\gamma} \left(\sqrt{A_\Lambda} V f_{\Gamma\gamma}^\dagger s_{0\Gamma\gamma} + \text{h.c.} \right) + \mathcal{H}_L^0, \quad (2.6)$$

$$\mathcal{H}_L^0 = \sum_{\ell=0}^{L-1} \sum_{\Gamma\gamma} t_\ell \left(s_{\ell+1\Gamma\gamma}^\dagger s_{\ell\Gamma\gamma} + \text{h.c.} \right), \quad (2.7)$$

where $s_{\ell\Gamma\gamma}$ is the annihilation operator of ℓ -th shell state with the γ -th component of the Γ -irreducible representation. The hopping energy, t_ℓ , between shell states is given by $t_\ell = D(1 + \Lambda^{-1})\Lambda^{-\ell/2}\xi_\ell/2$, where $\Lambda(> 1)$ is the discretization parameter, and ξ_ℓ tend to 1 when ℓ increases. The quantity A_Λ is the correction factor of order 1 for the discretization. We first diagonalize the \mathcal{H}_f term, and then by adding the shell state successively from $\ell = 0$, we diagonalize the series of cluster Hamiltonian, $\{\mathcal{H}_L\}$, recursively. At each step we retain about the 500 lower energy states to the next step. This number is not so large, but the obtained eigen states in the low energy region seem to have enough accuracy for qualitative discussions. When the only 300 states are retained at each step, the low energy eigen states are not changed essentially.

The valence of U ion in $U_x\text{Th}_{1-x}\text{Ru}_2\text{Si}_2$ is not so clear, so we consider two cases: one is the case that the valence fluctuation between $5f^2$ and $5f^1$ configurations becomes dominant, and the other is that between $5f^2$ and $5f^3$ configurations. We call the former a $f^2 - f^1$ dominant fluctuation case, and the latter a $f^2 - f^3$ dominant fluctuation case hereafter.

§3. Analysis of the Low Energy Fixed Point

3.1 Flow chart of energy levels of $f^2 - f^1$ dominant fluctuation case

We first consider the $f^2 - f^1$ dominant fluctuation case. We choose the parameters; $\varepsilon(\Gamma_7^{(1)}) = -0.9$, $\varepsilon(\Gamma_6) = -0.75$, $\varepsilon(\Gamma_7^{(2)}) = -0.5$, $U = 0.6$ and $I = 8$. The lowest CEF state becomes the non-Kramers doublet of the f^2 configuration which has mainly the character of $J = 4$, Γ_5 -irreducible representation of D_4 -group, and the energy of the state is -1.446 . The state is given as $|f^2\Gamma_5, \pm\rangle = a|\pm 1/2, \mp 3/2\rangle + b|\pm 3/2, \mp 5/2\rangle + c|\pm 5/2, \pm 1/2\rangle$, where $a = -0.3395$, $b = -0.1874$ and $c = 0.9218$. We have used the notation, $|m, m'\rangle \equiv f_m^\dagger f_{m'}^\dagger |0\rangle$, where m and m' are the magnetic quantum numbers of j . The excited states from the first to the forth are the singlet of the f^2 configuration with the energies, -1.442 , -1.286 , -1.208 and -1.167 , respectively. These states have mainly the character of $J = 4$, and are the Γ_4 , Γ_1 , Γ_2 and Γ_3 -irreducible representations of D_4 -group, respectively. The other configurations, f^0 and from f^3 to f^6 have higher energy.

In our previous work we have shown that three types of the ground state; the doublet, the CEF-singlet-like and the f^0 -singlet-like ground states appear successively when the hybridization strength is increased by fixing the energy of the CEF states.¹⁸⁾ The low energy spectrum of the last two

follows the LFL theory, however, the first one can not be explained by the LFL theory. In this work we concentrate on the weak hybridization case and analyze the spectrum of the NFL state. In Fig. 1 the lower eigen energies of each cluster Hamiltonian, \mathcal{H}_L , for the odd NRG step, L , are shown. The energies are renormalized by t_{L-1} at each step. The renormalized energy levels of the states which has the same charge, Q , and the magnetic quantum number, M , change smoothly, and we call the figure the flow chart of the renormalized energy levels (FCEL) hereafter. The quantity, M , is defined by using modulo 4 as defined in the caption of Fig. 1 because of the tetragonal symmetry. The renormalized energy levels tend to fixed values as L increases beyond a step $L \sim 23$. The right hand side of the figure gives the energy spectrum at the low energy fixed point, and the hopping energy, t_{L-1} , at $L \sim 23$ indicates the measure of the energy scale for the cross over that the system goes into the low energy fixed point. Each state is indicated by i (the sequential number of states from low to high energy), Q and M . The ground state ($i = 1, 2$) is doublet, and the first excited states are two doublet states with one particle excitation ($i = 3, 5$) and one hole excitation ($i = 4, 6$). The second excited states ($i = 7 \sim 10$) are the one hole excitation, and they have larger energy than twice energy of the first excited states. Therefore these low energy states can not be explained by the LFL theory.

We compare the low energy states with those of $S=1/2$ -TCKM which are derived by the conformal field theory (CFT).¹⁰⁾ The low energy states of $S=1/2$ -TCKM are the NFL states, and the energies for primary states are known as conformal towers,

$$E_{\text{CFT}}(Q_C, j, j_f) = \frac{v_F \pi}{\ell} \left\{ \frac{1}{8} \left(Q_C + 2 \frac{\delta_p}{\pi} \right)^2 + \frac{j(j+1)}{4} + \frac{j_f(j_f+1)}{4} \right\}, \quad (3.1)$$

where Q_C, j, j_f and δ_p denote the freedoms of the charge, the spin and the flavor-spin, and the potential scattering, respectively. As seen from the particle hole symmetry of the first excited states obtained by the NRG calculation, δ_p becomes zero. In Table I we compare the low energy states from the NRG calculation and those of the CFT. The renormalized energy, E , in the column of the NRG is multiplied by a constant factor, r^* , so the energy of the first excited states agrees with that of the CFT. The correspondence of the charge and the degeneracy between both results is perfect. The difference in energy is small for states in lower energy region with $r^*E \sim 0.5$, and it increases for ones in larger energy region, $r^*E \sim 1.0$. But the difference decreases when the discretization parameter, Λ in the NRG method, is decreased as shown in Fig. 2. It will disappear in the continuum limit, $\Lambda \rightarrow 1$. This behavior is the same as that of the $S=1/2$ -TCKM.²²⁾ It can be concluded the NFL part of the low energy spectrum in Fig. 1 has the same form to that of the $S=1/2$ -TCKM.

In the NRG calculation, we have low energy states which are not listed in Table I. They are explained as the states accompanied by the extra excitations obeying the LFL theory. In Table II

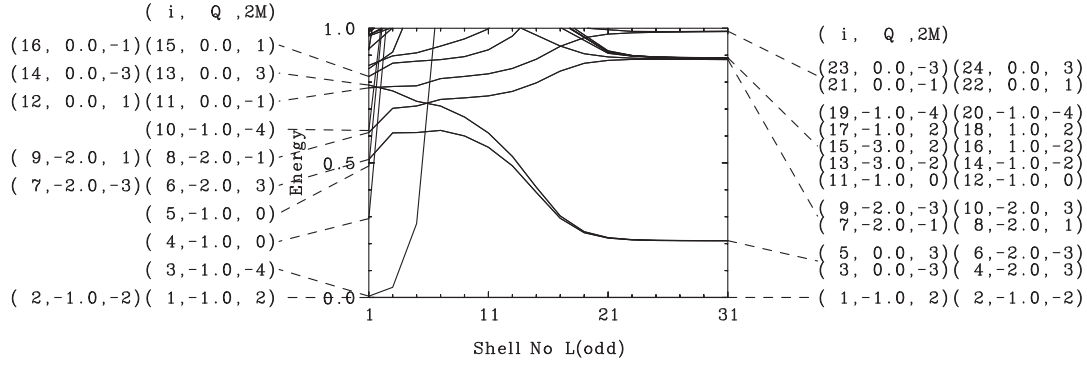


Fig. 1. FCEL of the $f^2 - f^1$ dominant fluctuation case for the odd renormalization step, L . (In this case the number of shell orbits for the conduction electrons is even, $L + 1$. For example, number of shell orbits is two for $L = 1$.) The energies are renormalized by t_{L-1} at each step. The discretization parameter $\Lambda = 8$ is used, and about 500 states are retained at each step. The parameters of IAM are; $\varepsilon(\Gamma_7^{(1)}) = -0.9$, $\varepsilon(\Gamma_6) = -0.75$, $\varepsilon(\Gamma_7^{(2)}) = -0.5$, $U = 0.6$, $I = 8$ and $V^2/2 = 0.035$. The occupation number of the f-electron is 1.92. Each state is labeled by the index, i (sequential number of states from low to high energy). The charge of each state is denoted by Q , which is defined as total electron number minus half of total orbital number, $3(L + 2)$. The magnetic quantum number, M is the index for grouping of total magnetic quantum number, J_z . When the quantity, $2J_z$ changes from $-4 + 8n$ to $3 + 8n$, where n is some integer, the quantity $2M$ varies from -4 to 3 . The renormalized energies of states which has the same Q and M are connected as L changed.

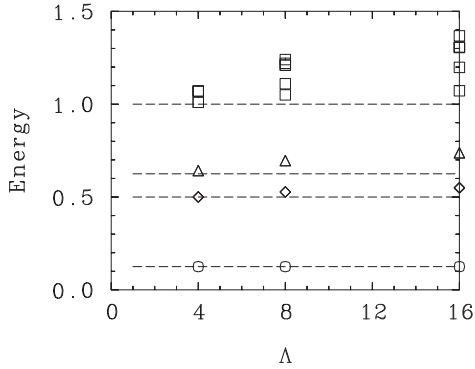


Fig. 2. Λ dependence of the energy belongs to the NFL part at the low energy fixed point. The symbols denote the renormalized energy, r^*E , given by the NRG calculation. The parameters are the same as those in Fig. 1 except V . The hybridization width is chosen as $V^2/2 = 0.0433$, 0.0350 and 0.0310 for the cases of $\Lambda = 4, 8$ and 16 , respectively. The dashed lines shows the energies which are expected by the CFT for the $S=1/2$ -TCKM. The factor, r^* , is chosen so each energy of the first excited state agrees with $1/8$; $r^* = 0.5787$, 0.5924 and 0.619 for $\Lambda = 4, 8$ and 16 , respectively.

Table I. Comparison between the states belong to the NFL part for the odd NRG step of the $f^2 - f^1$ dominant fluctuation case. The states at the low energy fixed point from the NRG calculation and the low energy states for the $S=1/2$ -TCKM expected from the CFT are listed. The parameters for the NRG calculation are the same as those in Fig. 1. The states in the column of NRG are the results at $L = 31$. Index in the column of NRG is the same in Fig. 1. The charge $Q - Q_0$, which is defined from in Fig. 1 and $Q_0 = -1$ of the ground state, coincides with Q_C . The degeneracy of each line in the column of CFT is given by $(2j + 1)(2j_f + 1)$, and it coincides with the degeneracy given by NRG. The energy, E , is multiplied by a factor $r^* = 0.5924$ which is defined so to agree the energy of the first excited state from the NRG and the CFT results. In the column of CFT the ground state energy, $3/16$, is subtracted.

index	NRG				CFT			
	$Q - Q_0$	degen.	E	r^*E	Q_C	j	j_f	$E_{\text{CFT}}\ell/\pi v_F$
1, 2	0	2	0	0	0	1/2	0	0
3, 5	1	2	0.211	0.125	1	0	1/2	1/8
4, 6	-1	2	0.211	0.125	-1	0	1/2	1/8
11, 12, 14, 17, 19, 20	0	6	0.889 ~ 0.891	0.527 ~ 0.528	0	1/2	1	1/2
13, 15	-2	2	0.890	0.527	-2	1/2	0	1/2
16, 18	2	2	0.890	0.527	2	1/2	0	1/2
33, 34, 39, 40, 43, 44	1	6	1.17 ~ 1.18	0.693 ~ 0.699	1	1	1/2	5/8
35-38, 41, 42	-1	6	1.17 ~ 1.18	0.693 ~ 0.699	1	1	1/2	5/8
55-58	0	4	1.77	1.05	0	3/2	0	1
79, 80	0	2	1.87	1.11	0	1/2	0	1
113, 114, 117-120	-2	6	2.05 ~ 2.06	1.21 ~ 1.22	-2	1/2	1	1
115, 116	0	2	2.06	1.22	0	1/2	0	1
121-126	0	6	2.06	1.22	0	1/2	1	1
153-158	2	6	2.10 ~ 2.11	1.24 ~ 1.25	2	1/2	1	1

we show the list of these states. The states, $i = 7 \sim 10$ and $i = 21 \sim 24$, are interpreted as the single particle excited state of the LFL part. The former (latter) are classified to the one hole (electron) excitation of the occupied (unoccupied) fermion orbitals with energy -0.884 (0.988). From the analysis of the magnetic quantum number the symmetry of the fermion orbitals of the LFL part is determined as Γ_7 . The NFL part for these eigen states is in its ground state, $i = 1$ and 2 . For the states from $i = 25$ to 52 in the Table II the NFL part is in the excited states, $i = 3 \sim 6$. Each state can be explained as the product of the NFL state and the LFL state. One can see the perfect correspondence of the charge and the magnetic quantum number between the NRG and the expected results. The energy in the column of LFL is estimated from the sum of the energies of the

NFL state and the LFL part.²³⁾ These energies give good agreement with those of the NRG, and thus the NFL and LFL parts seem to be almost independent with each other. The states, $i = 53$ and 54 , are interpreted as the two hole excited state of LFL part. The energies of the states agree with the sum of the energies of two holes as seen from Table II. This is the characteristic features of the LFL excitation. We have analyzed about 150 states as the product of the NFL state and the LFL one. In these state the particle-hole pair excitation or the two particles excitation of the LFL part are includes. It is concluded the low energy spectrum at the fixed point is explained by a model that is the combination of the NFL fixed point Hamiltonian and the LFL one which are independent with each other. However, we note the two parts have almost the same low energy scale because they tend to the low energy fixed point almost simultaneously at about $L \sim 23$ as seen from Fig. 1. We note the spectrum in the NFL part have the particle-hole symmetry, but there is the particle-hole asymmetry in the LFL part, so the total spectrum has the asymmetry.

In Fig. 3 we show the FCEL for the even renormalization step. The parameters are the same as those in Fig. 1. The energy flow is very complicated in the intermediate NRG step, but, the excitation spectrum at the larger step ($L > 26$) for the low energy fixed point is simple. The spectrum is explained by the same model as that for the odd renormalization step discussed above, that is the combination of the NFL fixed point model and the LFL one. The spectrum of the NFL part at the low energy fixed point has the same form as that for $S=1/2$ -TCKM as shown in Table III. The energy, E , has the same quantity as that of the odd NRG step. This is the characteristic behavior of the NFL state. In Table IV the low energy states including the excitation of the LFL part are shown. The states given by the NRG calculation can be explained by the combination of the LFL and the NFL states as shown in the column of LFL. The fermion orbitals have the Γ_7 symmetry. Only one orbital above the Fermi level is found even though we analyze about 150 states. The single hole excitation is expected to have an energy larger than 2.1.

There are three kinds of orbitals for the conduction electrons, $\Gamma_7^{(1)}$, $\Gamma_7^{(2)}$ and Γ_6 . Two of them will contribute to the NFL state, and remaining one will be left as the LFL part. To find which orbitals are related to the NFL state, we consider a fictitious model that the conduction electrons with the $\Gamma_7^{(1)}$ symmetry are removed from the original model given in eq. (2.1). In Fig. 4 the FCEL of the fictitious model is shown. At the low energy fixed point the energy spectrum does not depend on whether the NRG step is odd or even. The low energy spectrum is almost the same as that of the NFL part of the original model. There are the small particle-hole asymmetry in the spectrum of the fictitious model. All the states at the low energy fixed point can be analyzed as the conformal towers of the $S=1/2$ -TCKM with the potential scattering term. The conduction electrons with Γ_6 and $\Gamma_7^{(2)}$ symmetries contribute to the NFL state, and the electrons with $\Gamma_7^{(1)}$ to the LFL state.

Table II. Comparison between the states belong to the LFL part for odd NRG step of the f^2 - f^1 dominant fluctuation case. The states at the low energy fixed point from the NRG calculation and the low energy states which is expected by the LFL theory are listed. The parameters for the NRG calculation are the same as those in Fig. 1. The quantities, Q , M and energy in the column of NRG is the results for $L = 31$ in Fig. 1. All the states in NRG can be explained by the product of the NFL state and the single particle state which is indicated in the column of LFL. The NFL state is indicated by $[\text{NFL}(i)]$, where i is the index of the state shown in Fig. 1 and in Table I. The single particle state is indicated by $\Gamma_{7(1)}^+$ and $\Gamma_{7(1)}^-$, where the plus (minus) sign means the particle (hole) excitation. The two hole excited state is indicated by $[\Gamma_{7(1)}^-]^2$. The excitation energies, $E(\Gamma_{7(1)}^+)$ and $E(\Gamma_{7(1)}^-)$, is given as 0.988 and 0.844, respectively, to agree with those in the column of NRG. The energy in the column of LFL is estimated from the sum of the NFL state energy and the single particle excitation energy.

index	NRG			LFL	
	Q	$2M$	energy	state	energy
7, 9	-2	-1, -3	0.884	$[\text{NFL}(1)] \otimes \Gamma_{7(1)}^-$	0.884
8, 10	-2	1, 3	0.884	$[\text{NFL}(2)] \otimes \Gamma_{7(1)}^-$	0.884
21, 23	0	-1, -3	0.988	$[\text{NFL}(1)] \otimes \Gamma_{7(1)}^+$	0.988
22, 24	0	1, 3	0.988	$[\text{NFL}(2)] \otimes \Gamma_{7(1)}^+$	0.988
25, 29	-2	0, -2	1.096	$[\text{NFL}(4)] \otimes \Gamma_{7(1)}^-$	1.095
26, 30	-3	0, 2	1.096	$[\text{NFL}(6)] \otimes \Gamma_{7(1)}^-$	1.095
27, 31	-1	2, 0	1.096	$[\text{NFL}(3)] \otimes \Gamma_{7(1)}^-$	1.095
28, 32	-1	-2, 0	1.096	$[\text{NFL}(5)] \otimes \Gamma_{7(1)}^-$	1.095
45, 49	1	0, 2	1.200	$[\text{NFL}(3)] \otimes \Gamma_{7(1)}^+$	1.199
46, 50	1	0, 2	1.200	$[\text{NFL}(5)] \otimes \Gamma_{7(1)}^+$	1.199
47, 51	-1	-2, 0	1.201	$[\text{NFL}(4)] \otimes \Gamma_{7(1)}^+$	1.199
48, 52	-1	2, 0	1.201	$[\text{NFL}(6)] \otimes \Gamma_{7(1)}^+$	1.199
53	-3	2	1.768	$[\text{NFL}(1)] \otimes [\Gamma_{7(1)}^-]^2$	1.768
54	-3	-2	1.768	$[\text{NFL}(2)] \otimes [\Gamma_{7(1)}^-]^2$	1.768

When we consider a fictitious model that the conduction electrons with the Γ_6 or $\Gamma_7^{(2)}$ symmetry are removed, the low energy states are explained by a Ising type model: One localized Ising spin couples with the conduction electrons through the exchange interaction.

3.2 Flow chart of energy levels of f^2 - f^3 dominant fluctuation case

For the f^2 - f^3 dominant fluctuation case we choose the parameters; $\varepsilon(\Gamma_7^{(1)}) = -1.2$, $\varepsilon(\Gamma_6) = -1.05$, $\varepsilon(\Gamma_7^{(2)}) = -0.8$, $U = 0.3$ and $I = 8$. The f -levels is chosen to be deeper and the Coulomb interaction

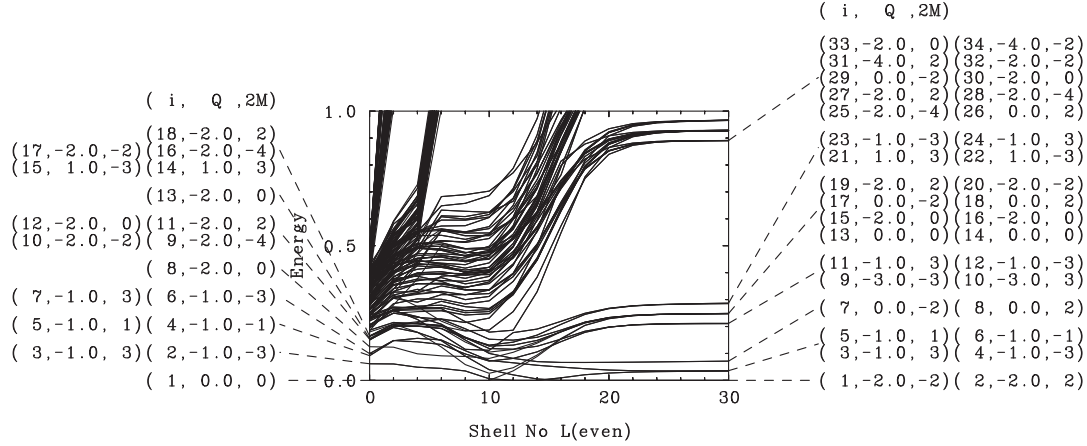


Fig. 3. FCEL of the $f^2 - f^1$ dominant fluctuation case for the even renormalization step L . The parameters for the NRG calculation are the same as those in Fig. 1. See the caption of Fig. 1.

to be smaller than those for the $f^2 - f^1$ dominant fluctuation case with fixing the CEF splitting of f -level and the exchange interaction. The main states of the f^2 configuration are almost the same as those of the previous case. The lowest CEF state is the non-Kramers doublet which has the energy, -2.346 , and it has mainly the character of $J = 4$, Γ_5 -irreducible representation of D_4 -group. The first to the fourth excited states are the singlet which has mainly the character of Γ_4 , Γ_1 , Γ_2 and Γ_3 -irreducible representation of D_4 -group, respectively. The energy of each state is -2.342 , -2.186 , -2.108 and -2.067 , respectively. The main states of the f^3 configuration have mainly the character of $J = 9/2$. They are the Γ_6 doublet, the Γ_7 doublet and the another Γ_7 doublet states with energies -1.958 , -1.927 and -1.907 , respectively. When the hybridization matrix $\Gamma = \pi V^2/2$ is changed from 0.030π to 0.038π for $\Lambda = 8$, the occupation number of the f -electron varied from 2.233 to 2.255.

In Fig. 5 (a) the FCEL for the odd NRG step is shown. Each energy spectrum at the low energy fixed point is explained by the combination of the NFL fixed point Hamiltonian and the LFL one which are independent with each other also in this case. In Table V we show the comparison between the low energy states in the NFL part of the NRG result and those of the conformal tower of $S=1/2$ -TCKM. The first excited state is the one-particle excitation doublet ($i = 3, 4$), and the second excited state is the one-hole excitation doublet ($i = 5, 6$). There exists the particle-hole asymmetry, so the multiplying factor, $r^* = 0.592$, and the potential scattering, $\delta_p = -0.235$, are determined from the first and the second excited states. The states of the NRG result show good correspondence to the result of CFT. We note the difference of the energies has comparable magnitude as that found in Table I. It decreases when we use $\Lambda = 4$, and it will be removed in the continuum limit, $\Lambda \rightarrow 1$. The states accompanied by the LFL excitation are not listed in the

Table III. Comparison between the states belong to the NFL part for even NRG step of the $f^2 - f^1$ dominant fluctuation case. The states at the low energy fixed point from the NRG calculation and the low energy states for the $S=1/2$ -TCKM expected from the CFT are listed. The parameters for the NRG calculation are the same as those in Fig. 1. The states in the column of NRG are the results at $L = 30$. The multiplying factor is $r^* = 0.5924$. In the column of CFT the ground state energy, $3/16$, is subtracted. See the caption of Table I.

index	NRG				CFT			
	$Q - Q_0$	degen.	E	r^*E	Q_C	j	j_f	$E_{\text{CFT}}\ell/\pi v_F$
1, 2	0	2	0	0	0	1/2	0	0
9, 10	-1	2	0.211	0.125	-1	0	1/2	1/8
11, 12	1	2	0.211	0.125	1	0	1/2	1/8
25, 27, 28, 30, 32, 33	0	6	0.891	0.528	0	1/2	1	1/2
26, 29	2	2	0.891	0.528	2	1/2	0	1/2
31, 34	-2	2	0.891	0.528	-2	1/2	0	1/2
65-70	-1	6	1.17 ~ 1.18	0.693 ~ 0.699	-1	1	1/2	5/8
71-76	1	6	1.18	0.699	1	1	1/2	5/8
113-116	0	4	1.77	1.05	0	3/2	0	1
129, 130, 135, 136, 147, 148	-2	6	2.10 ~ 2.11	1.24 ~ 1.25	-2	1/2	1	1
131-134, 145, 146	0	6	2.11	1.25	0	1/2	1	1
137-139, 141, 143, 144	2	6	2.11	1.25	2	1/2	1	1
140, 142	0	2	2.11	1.25	0	1/2	0	1

table. The LFL states are explained as the excitations of the orbital with the Γ_7 symmetry. This situation is common to the $f^2 - f^1$ dominant fluctuation case.

In Fig. 5 (b) we show the FCEL for the even NRG step. The NFL part of the low energy states are listed in Table VI. The quantities, r^* and δ_p , don't depend on the even or oddness of the NRG step. The LFL part is not listed in the table. The first excited states which are indicated by the index, $i = 3 \sim 6$, in the right hand side of the figure are the one hole excitations of the fermion orbital with Γ_7 symmetry from the ground state doublet in the NFL part. The second excited states are the two holes excitations from the ground state. As seen from the figure there are the one hole excitations and the two holes excitations of the LFL part from each NFL state.

When we consider the fictitious model that the conduction electrons with $\Gamma_7^{(1)}$ symmetry are removed, the spectrum at the low energy shows a similar NFL behavior of the original model. In other cases; the fictitious model removing the conduction electrons with the Γ_6 or $\Gamma_7^{(2)}$ symmetry, we have the Ising type fixed point. Therefore the Γ_6 and $\Gamma_7^{(2)}$ components contribute to the NFL

Table IV. Comparison between the states belong to the LFL part for even NRG step of the $f^2 - f^1$ dominant fluctuation case. The states at the low energy fixed point from the NRG calculation and the low energy states which is expected by the LFL theory are listed. The parameters for the NRG calculation are the same as those in Fig. 1. The quantities in the column of NRG are the results for $L = 30$ in Fig. 3. The NFL state is indicated by $[\text{NFL}(i)]$, where i is the index of the state shown in Fig. 3 and in Table III. See the caption of Table II.

index	NRG			LFL	
	Q	$2M$	energy	state	energy
3, 5	-1	3, 1	0.0345	$[\text{NFL}(1)] \otimes \Gamma_{7(1)}^+$	0.0345
4, 6	-1	-3, -1	0.0345	$[\text{NFL}(2)] \otimes \Gamma_{7(1)}^+$	0.0345
7	0	-2, 2	0.0714	$[\text{NFL}(1)] \otimes 2\Gamma_{7(1)}^+$	0.0690
8	0	2, 2	0.0715	$[\text{NFL}(2)] \otimes 2\Gamma_{7(1)}^+$	0.0690
13, 17	0	0, -2	0.248	$[\text{NFL}(11)] \otimes \Gamma_{7(1)}^+$	0.246
14, 18	0	0, 2	0.248	$[\text{NFL}(12)] \otimes \Gamma_{7(1)}^+$	0.246
15, 19	-2	0, 2	0.248	$[\text{NFL}(9)] \otimes \Gamma_{7(1)}^+$	0.246
16, 20	-2	0, -2	0.248	$[\text{NFL}(10)] \otimes \Gamma_{7(1)}^+$	0.246
21	1	3	0.285	$[\text{NFL}(11)] \otimes [\Gamma_{7(1)}^+]^2$	0.280
22	1	-3	0.285	$[\text{NFL}(12)] \otimes [\Gamma_{7(1)}^+]^2$	0.280
23	-1	-3	0.287	$[\text{NFL}(9)] \otimes [\Gamma_{7(1)}^+]^2$	0.280
24	-1	3	0.287	$[\text{NFL}(10)] \otimes [\Gamma_{7(1)}^+]^2$	0.280

part and the $\Gamma_7^{(1)}$ to the LFL part. This fact is the same as that of the $f^2 - f^1$ dominant fluctuation case.

We note when the original model with the large hybridization strength is considered, the low energy states are explained by the LFL theory. The lowest energy state at each NRG step changes from the crystalline field doublet ($L = -1$) to the singlet state ($L \geq 15$) in the FCEL of the odd step. The two electrons are bounded at the intermediate step, $L = 15$, so the singlet state has the character similar to that of the f^4 singlet state. This contrasts with the f^0 -singlet-like ground state in the $f^2 - f^1$ dominant fluctuation case with the large hybridization strength.

From the analysis of this section we can deduce the following conclusions: The low energy fixed point properties of the present model can be given by the combination of the two independent parts, one is the NFL component and the another is the LFL component. The two parts have almost the same low energy scale, and in addition the separation of these occurs at almost the same energy region with the low energy scale. The conduction electrons with Γ_6 and $\Gamma_7^{(2)}$ symmetry contribute to the NFL part and the $\Gamma_7^{(1)}$ symmetry to the LFL part. The above facts are seen commonly both

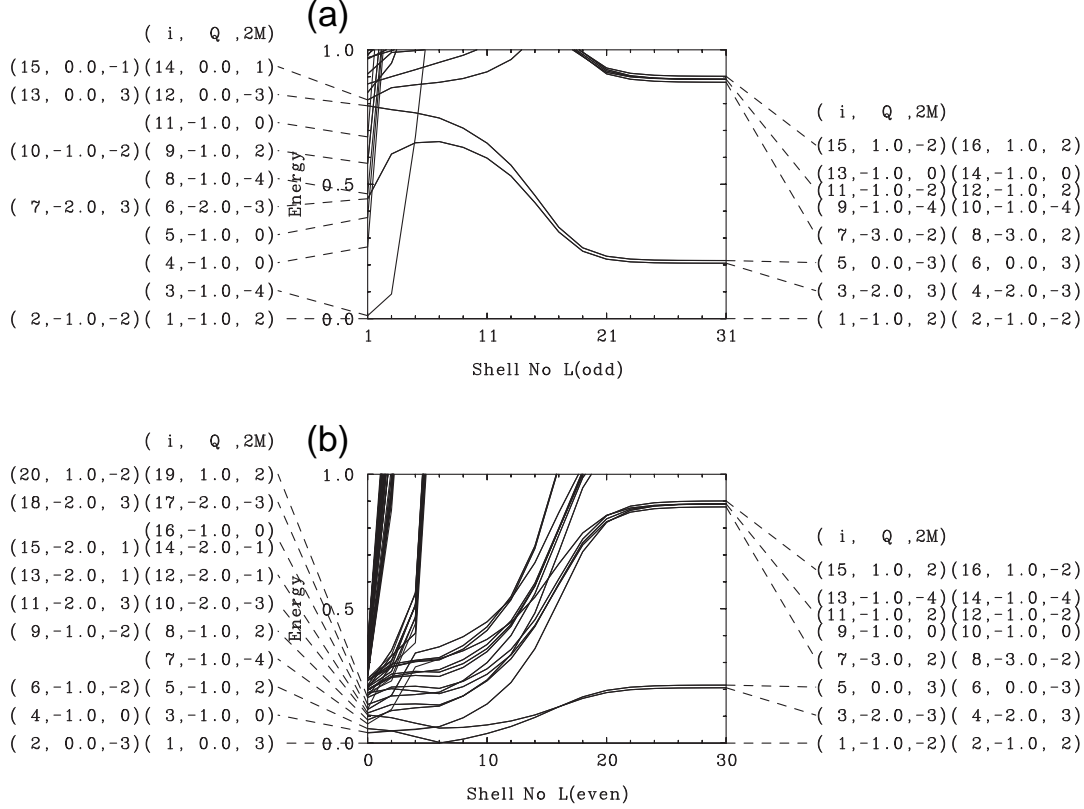


Fig. 4. FCEL of the fictitious model for the odd (a) and even (b) renormalization steps L . The parameters for the NRG calculation are the same as those in Fig. 1. See the caption of Fig. 1.

for the $f^2 - f^1$ and the $f^2 - f^3$ fluctuation cases.

§4. Magnetization

We calculate the temperature dependence of the magnetization of f-electrons, $M = \langle m_f \rangle = \langle \sum_{m=-j}^j m f_m^\dagger f_m \rangle$, by adding the Zeeman term, $\mathcal{H}' = -m_f H_z$, to eq. (2.1), where m is the magnetic quantum number of j . The thermal average at the temperature, T_L , is calculated by the eigen states of the L th cluster as,

$$M(T_L) = \frac{\text{Tr} m_f \exp \{ -(\mathcal{H}_L + \mathcal{H}') / T_L \}}{\text{Tr} \exp \{ -(\mathcal{H}_L + \mathcal{H}') / T_L \}}, \quad (4.1)$$

$$T_L = \frac{1}{2} (1 + \Lambda^{-1}) \Lambda^{(L-1)/2} / \bar{\beta}, \quad (4.2)$$

where $\bar{\beta} \sim 2$ is a parameter for suiting the temperature to the eigen energies of each NRG step.

In Fig. 6 (a) we show the magnetizations which are normalized by the applied magnetic fields. These quantities correspond to the magnetic susceptibility when the field is weak enough. The pa-

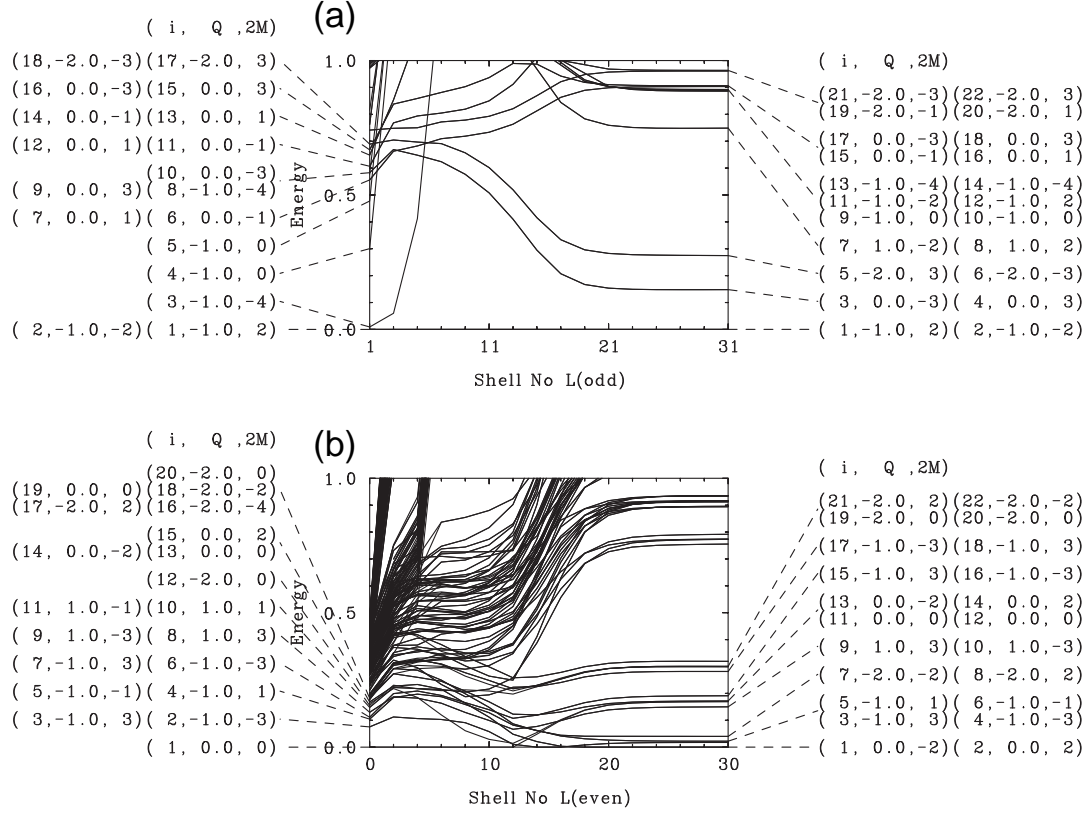


Fig. 5. FCEL of the $f^2 - f^3$ dominant fluctuation case for the odd (a) and the even (b) renormalization steps L . The discretization parameter $\Lambda = 8$ is used, and about 500 states are retained at each step. The parameters of IAM are; $\varepsilon(\Gamma_7^{(1)}) = -1.2$, $\varepsilon(\Gamma_6) = -1.05$, $\varepsilon(\Gamma_7^{(2)}) = -0.8$, $U = 0.3$, $I = 8$ and $V^2/2 = 0.036$. The occupation number of the f -electron becomes 2.21. See the caption of Fig. 1.

parameters of the IAM are chosen so that the valence fluctuation between the f^2 and f^3 configurations becomes dominant. We use $\Lambda = 8$ and about 400 states are kept at each NRG step. Even when we keep about 500 states, the results of the magnetization are not changed essentially. The normalized magnetizations have almost same value, when the temperature is higher than the Zeeman energy. For very weak magnetic field there is a temperature region that the magnetization follows the $-\ln T$ dependence. When the temperature decreases, the magnetization saturates. However, $-\ln T$ temperature region extends with decreasing the applied magnetic field. This behavior can be seen clearly from Fig. 6 (b) which shows the differential of the magnetizations by the logarithm of the temperature. The magnetic susceptibility follows $-\ln T$ dependence at low temperatures. This temperature dependence is the characteristic behavior of the NFL state for $S=1/2$ -TCKM type. The inverse of the coefficient of $-\ln T$ term is estimated to be about 10^{-7} . This means that

Table V. Comparison between the states belong to the NFL part for the odd NRG step of the $f^2 - f^3$ dominant fluctuation case. The states at the low energy fixed point from the NRG calculation and the low energy states for the $S=1/2$ -TCKM expected from the CFT are listed. The parameters for the NRG calculation are the same as those in Fig. 5. The states in the column of NRG are the results at $L = 31$. The multiplying factor, $r^* = 0.5920$, and the potential scattering, $\delta_p = -0.2350$, are defined to agree the energies of the first and the second excited states from the NRG and the CFT results. In the column of CFT the ground state energy, $(\pi\delta_p/2)^2 + 3/16$, is subtracted. See the caption of Table I.

index	NRG				CFT			
	$Q - Q_0$	degen.	E	r^*E	Q_C	j	j_f	$E_{\text{CFT}}\ell/\pi v_F$
1, 2	0	2	0	0	0	1/2	0	0
3, 4	1	2	0.148	0.0876	1	0	1/2	0.0876
5, 6	-1	2	0.274	0.162	-1	0	1/2	0.162
7, 8	2	2	0.749	0.443	2	1/2	0	0.425
9-14	0	6	0.889 \sim 0.892	0.524 \sim 0.528	0	1/2	1	1/2
23, 24	-2	2	1.03	0.610	-2	1/2	0	0.575
29-34	1	6	1.09 \sim 1.10	0.645 \sim 0.648	1	1	1/2	0.588
47-52	-1	6	1.26 \sim 1.27	0.748 \sim 0.749	-1	1	1/2	0.662

the energy scale which characterizes the strength of the $-\ln T$ term of the susceptibility is about 10^{-7} , and is very small. Therefore the present model gives sizable $-\ln T$ term.

The saturation of the magnetization relates to a break of the NFL state under the magnetic field as follows: In Fig. 7 the FCEL for the odd NRG step under the magnetic field, $H_z = 1.0 \times 10^{-9}$, is shown. The energy flow in the region below $L = 15$ is almost identical to that in Fig. 5(a) which is the FCEL without the magnetic field. The spectrum for $L = 15 \sim 21$ splits gradually due to the magnetic field. However, the behavior is very similar to that of the NFL spectrum at the low energy fixed point in Fig. 5 (a). The hopping energy at $L = 21$, $t_{L-1} \sim \Lambda^{-10} \sim 10^{-9}$, has the same order to that of the Zeeman energy. We note that the magnetization shows the saturation deviated from the $-\ln T$ behavior at about $T \sim 10^{-10}$ for the case of $H_z = 10^{-9}$. The flow in the region above $L = 21$ goes to the LFL spectrum at the low energy fixed point. The first and second excited states, $i=2$ and 3, where i is the index in the figure, are the one electron excitations, respectively. The third ($i=4$) and fourth ($i=5$) excited states are the one hole excitations. The excited state, $i=6$, is the two electrons excitation which is explained by the combination of the excitations for the states, $i=2$ and 3. The excited states, $i = 7 \sim 9$, are explained by the electron-hole pair excitations, and other high energy states are also explained by the LFL fixed point model. The NFL state breaks

Table VI. Comparison between the states belong to the NFL part for the even NRG step of the $f^2 - f^3$ dominant fluctuation case. The states at the low energy fixed point from the NRG calculation and the low energy states for the $S=1/2$ -TCKM expected from the CFT are listed. The parameters for the NRG calculation are the same as those in Fig. 5. The states in the column of NRG are the results at $L = 30$. The multiplying factor and the potential scattering are: $r^* = 0.5799$ and $\delta_p = -0.2393$, respectively. In the column of CFT the ground state energy, $(\pi\delta_p/2)^2 + 3/16$, is subtracted. See the caption of Table I.

index	NRG				CFT			
	$Q - Q_0$	degen.	E	r^*E	Q_C	j	j_f	$E_{\text{CFT}}\ell/\pi v_F$
1, 2	0	2	0	0	0	1/2	0	0
9, 10	1	2	0.150	0.0869	1	0	1/2	0.0869
17, 18	-1	2	0.281	0.163	-1	0	1/2	0.163
25, 26	2	2	0.755	0.447	2	1/2	0	0.424
33-38	0	6	0.894 ~ 0.896	0.529 ~ 0.530	0	1/2	1	1/2
57, 58	-2	2	1.04	0.614	-2	1/2	0	0.576
65-70	1	6	1.10 ~ 1.10	0.649	1	1	1/2	0.587
89-94	-1	6	1.27	0.750	-1	1	1/2	0.663

due to the magnetic field, and the low energy states can be explained by the LFL theory.

In Fig. 8 we show the magnetizations for the NFL states of various parameter cases. It is normalized by a quantity, M^* , where M^* is the magnetization under very weak magnetic field at a temperature, T^* . The quantity, T^* is defined as the temperature that $-\ln T$ dependence of the magnetization begins. The strength of the $-\ln T$ term is approximately characterized by $1/T^*$. The symbols shows the magnetizations for the $f^2 - f^3$ dominant fluctuation case, and the lines for the $f^2 - f^1$ dominant fluctuation one. As seen from the figure the normalized magnetizations under the same normalized magnetic field, H_z/T^* have almost the same temperature dependence. When the magnetic field is very weak, the temperature region that the magnetization has the $-\ln T$ dependence spreads from T^* to $H_z/10$. The model of the $f^2 - f^1$ dominant fluctuation also gives sizable $-\ln T$ divergence.

§5. Magneto Resistance

In the previous sections we have shown that the low energy spectrum of the present model is formed by the combination of the NFL and the LFL parts. We note that the phase shift which is

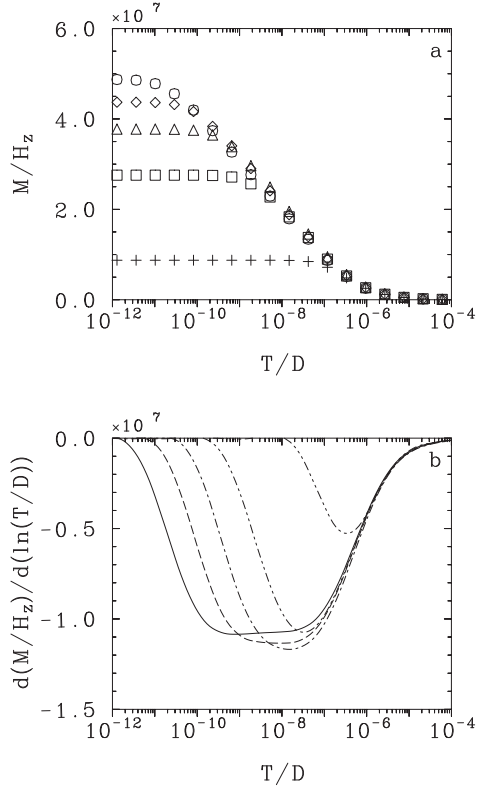


Fig. 6. Temperature dependence of the normalized magnetizations (a) and the differential of them by the logarithm of the temperature (b) for several magnetic fields, $H_z = 1 \times 10^{-9}$ (o, solid line), 2×10^{-9} (◊, dashed line), 4×10^{-9} (△, dot-dashed line), 1×10^{-8} (□, two-dots-dashed line), and 1×10^{-7} (+, three-dots-dashed line), respectively. The parameters are chosen so that the valence fluctuation between the f^2 and f^3 configurations becomes dominant: $\varepsilon(\Gamma_7^{(1)}) = -1.2$, $\varepsilon(\Gamma_6) = -1.05$, $\varepsilon(\Gamma_7^{(2)}) = -0.8$, $U = 0.3$, $I = 8$ and $V^2/2 = 0.035$. The occupation number of the f -electron for $H_z = 1 \times 10^{-9}$ is 2.23. $\Lambda = 8$ is used, and about 400 states are retained at each renormalization step.

calculated from the spectra of LFL part becomes very small at low energy fixed point. Therefore the electric resistivity caused by the LFL part will decrease with decreasing temperature. In this section we study the electric resistivity due to the NFL part. To simplify the analysis we use the fictitious model which is introduced in §3.2. When the magnetic field is applied, the spectrum at the low energy fixed point follows the LFL theory. The single particle excitations are given by the following effective Hamiltonian,

$$\begin{aligned} \mathcal{H}^{\text{eff}} = & \mathcal{H}_L^0 + \sum_{\Gamma\gamma} \delta_f^{\text{eff}}(\Gamma\gamma) f_{\Gamma\gamma}^\dagger f_{\Gamma\gamma} \\ & + \sum_{\Gamma\gamma} \sqrt{2\Gamma_\Lambda^{\text{eff}}(\Gamma\gamma)/\pi} \left(f_{\Gamma\gamma}^\dagger s_{0\Gamma\gamma} + \text{h.c.} \right), \end{aligned} \quad (5.1)$$

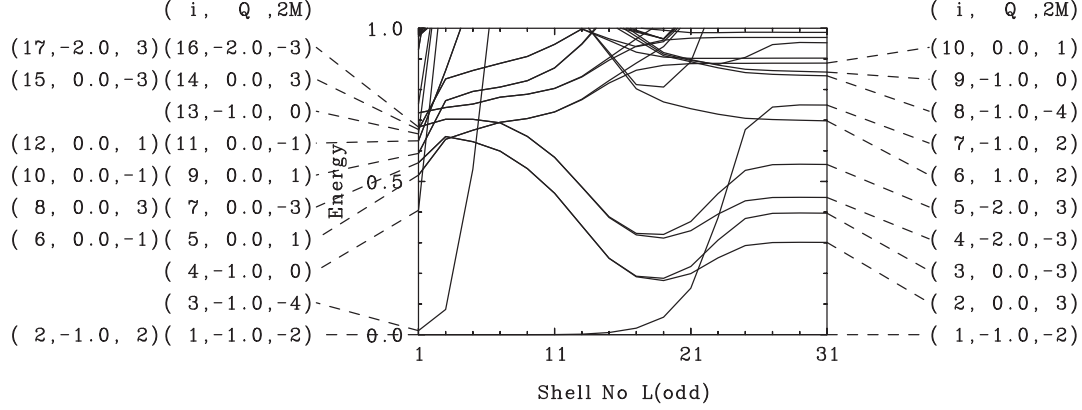


Fig. 7. FCEL under the magnetic field, $H_z = 1 \times 10^{-9}$ for the odd renormalization steps L . The parameters are the same as those in Fig. 6. See the caption of Fig. 1.

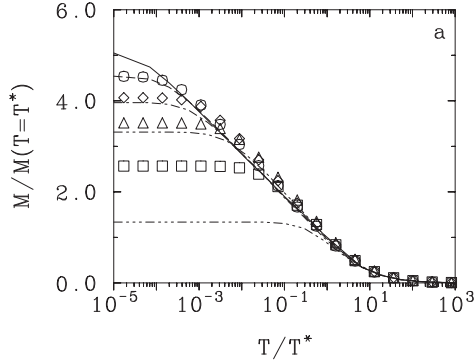


Fig. 8. Temperature dependence of scaled magnetizations for several magnetic fields. $\Lambda = 8$ is used, and about 400 states are kept in each renormalization step. The parameters for the magnetizations, which are indicated by the symbols, are $\varepsilon(\Gamma_7^{(1)}) = -1.2$, $\varepsilon(\Gamma_6) = -1.05$, $\varepsilon(\Gamma_7^{(2)}) = -0.8$, $U = 0.3$, $I = 8$ and $V^2/2 = 0.035$, and $H_z/T^* = 1.35 \times 10^{-2}$ (\circ), 2.7×10^{-2} (\diamond), 5.4×10^{-2} (\triangle) and 0.135 (\square), where $T^* = 7.42 \times 10^{-8}$. The occupation number of the f-electron for $H_z/T^* = 1.35 \times 10^{-2}$ is 2.23. The magnetizations are normalized by $M^* \equiv M(T = T^*, H_z = 1 \times 10^{-9}) = 1.07 \times 10^{-3}$. The parameters for the magnetizations which are indicated by the lines are $\varepsilon(\Gamma_7^{(1)}) = -0.9$, $\varepsilon(\Gamma_6) = -0.75$, $\varepsilon(\Gamma_7^{(2)}) = -0.5$, $U = 0.6$, $I = 8$ and $V^2/2 = 0.035$, and $H_z/T^* = 5.5 \times 10^{-3}$ (solid line), 1.1×10^{-2} (dashed line), 2.2×10^{-2} (dot-dashed line), 5.5×10^{-2} (two-dot-dashed line) and 0.55 (three-dot-dashed line), where $T^* = 1.82 \times 10^{-8}$. The occupation number of the f-electron for $H_z/T^* = 5.5 \times 10^{-3}$ is 1.91. $M^* \equiv M(T = T^*, H_z = 1 \times 10^{-10}) = 4.74 \times 10^{-3}$.

where $\delta_f^{\text{eff}}(\Gamma\gamma)$ and $\Gamma_\Lambda^{\text{eff}}(\Gamma\gamma)$ are the effective single particle level and effective hybridization width, respectively.²¹⁾ The effective quantities depend on the Γ and the suffix γ specifying its component, and are determined by using the low energy excited states. The phase shift is given as,

$$\eta(\Gamma\gamma) = \frac{\pi}{2} + \arctan \frac{-\delta_f^{\text{eff}}(\Gamma\gamma)}{\Gamma_\Lambda^{\text{eff}}(\Gamma\gamma)/A_\Lambda}. \quad (5.2)$$

Figure 9 shows the magnetic fields dependence of the phase shift. The hybridization strength is increased from Figs. (a) to (c). We note even though the hybridization is large in Fig. (c), the low energy spectrum follows the NFL model for the case of no magnetic field. Each symbol shows the phase shift for each component of the Γ -irreducible representation. When the hybridization is weak, phase shift has the values about $\pi/4$ and $3\pi/4$ at weak magnetic field limit. This behavior is same to that of $S=1/2$ -TCKM.²²⁾ When the magnetic field is increased, the phase shift changes gradually, and the strength of the scattering amplitude for all components decreases. In the case of the intermediate hybridization, the phase shift scarcely depends on the magnetic field. When the magnetic field is increased in the case of the large hybridization, the phase shift of three components changes to increase the strength of the scattering amplitude, while that of one component changes to decrease it.

We calculate the magneto resistance by assuming that four components contribute with equal weight,

$$R(H_z) = \sum_{\Gamma\gamma} (1 - \cos 2\eta(\Gamma\gamma)). \quad (5.3)$$

Figure 10 shows the magneto resistance at $T = 0$, where the circle, diamond and triangle are calculated from the phase shift shown in Figs. 9(a), (b) and (c), respectively. Each resistance goes to 4.0 in the weak magnetic field limit. This value is half of the unitarity limit value. When the hybridization is small, we have the negative magneto resistance, while we have the positive magneto resistance for the large hybridization case. The magnetization for the case of large hybridization is shown in Fig. 11. We can see the $-\ln T$ dependence with the large coefficient. The coefficient of the $-\ln T$ term is large also for the small hybridization case. When the hybridization is intermediate, the resistance hardly depends on the magnetic field, and the temperature, T^* , becomes high. This indicates that the initial; namely, the non-renormalized model is close to the low energy fixed point model. We note that the coefficient of the $-\ln T$ term is small in this case.

We note that the positive magneto resistance is recently observed at low temperature for $U_x\text{Th}_{1-x}\text{Ru}_2\text{Si}_2$.²⁴⁾ For the positive magneto resistance case we can expect that the electric resistivity decreases with decreasing temperature. In fact, Affleck *et al.* have demonstrated that the magneto resistance is positive for the $S=1/2$ -TCKM with very strong exchange coupling case.²²⁾ In this case we can expect that the resistivity decreases with decreasing temperature. The renormalized coupling decreases with decreasing temperature for the strong coupling model because the low energy fixed point of the NFL state is characterized by the intermediate coupling value. We

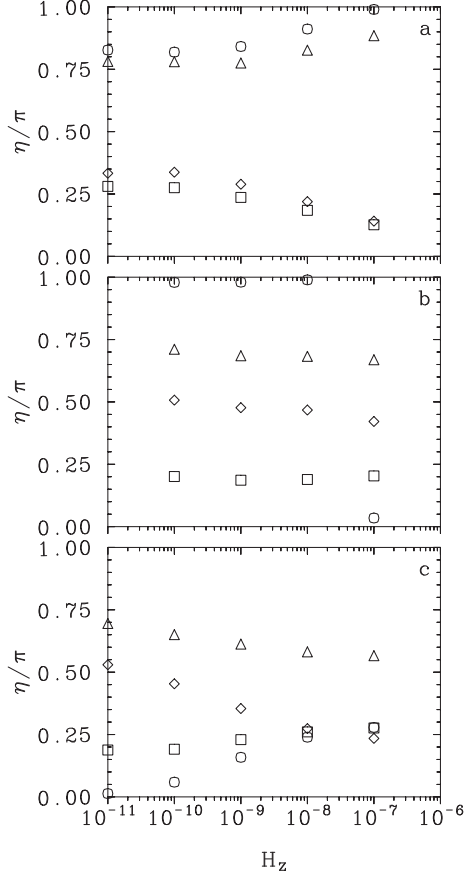


Fig. 9. Magnetic field dependence of the phase shift. The parameters are $\varepsilon(\Gamma_7^{(1)}) = -1.2$, $\varepsilon(\Gamma_6) = -1.05$, $\varepsilon(\Gamma_7^{(2)}) = -0.8$, $U = 0.3$, $I = 8$ and $V^2/2 = 0.035$ (a), 0.13 (b) and 0.16 (c). The occupation number of the f-electron for $H_z = 0$ are 2.11 (a), 2.27 (b) and 2.29 (c), respectively. Each symbol shows the phase shift for each component of the Γ -irreducible representation; $[\Gamma_7, +]$ (\circ), $[\Gamma_7, -]$ (\diamond), $[\Gamma_6, +]$ (\triangle) and $[\Gamma_6, -]$ (\square).

can also expect the positive magneto resistance when the low energy fixed point of the NFL state is approached from the stronger coupling side with renormalization step. The larger hybridization case of the present model seems to show this situation. We note that the present model can give the positive magneto resistance together with the sizable $-\ln T$ term of the magnetic susceptibility. However, the $S=1/2$ -TCKM has very small coefficient of the $-\ln T$ term with magnitude, $1/D$, because the exchange constant must have comparable value with the band width to get the positive magneto resistance.

From the calculations shown in this section we can expect that the anomalous properties of $U_x\text{Th}_{1-x}\text{Ru}_2\text{Si}_2$ can be explained within the scenario of the NFL anomaly of the TCKM type. Here we note the temperature dependence of the resistivity of the ETCAM. The resistivity of the

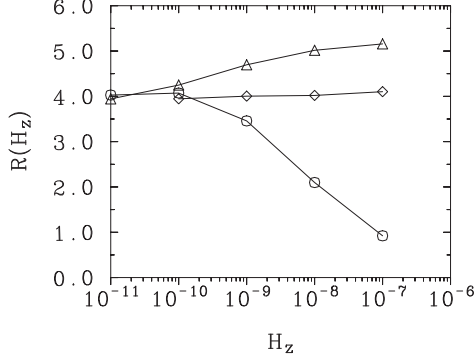


Fig. 10. Magneto resistance for the several cases of hybridization strength. The parameters are the same as those in Fig. 9 a (o), b (◇) and c (△).

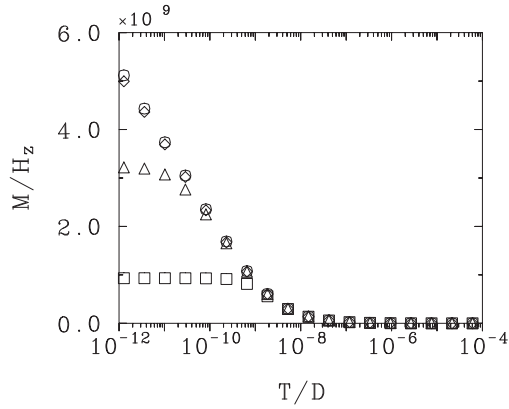


Fig. 11. Temperature dependence of the normalized magnetizations for the positive magneto resistance case. The parameters are the same as those in Fig. 9 (c). The magnetic fields are $H_z = 1 \times 10^{-12}$ (o), 2×10^{-11} (◇), 4×10^{-10} (△) and 1×10^{-9} (□), respectively.

ETCAM decreases with decreasing temperature, when the large hybridization is assumed.¹⁴⁾ In the very low energy region of the NFL state, the scattering amplitude decreases to half of the unitarity limit value from the larger value (near the unitarity limit) of the preceding energy region. The preceding region is characterized by the Kondo effect of the two-channel Anderson model with larger hybridization. The behavior of the FCEL of the ETCAM have similar characteristics to that of the present model with larger hybridization. It shows the temperature dependence of the magnetization and the resistivity similar to that of $U_x\text{Th}_{1-x}\text{Ru}_2\text{Si}_2$. The ETCAM seems to be an effective model of the NFL part of the realistic model at low temperature. The local spin in

the ETCAM will correspond to the f-electron with $\Gamma_7^{(1)}$ symmetry, while the two channels will correspond to electrons with $\Gamma_7^{(2)}$ and Γ_6 symmetries of the present model. However, at present it is not easy to relate the interaction terms between two models.

§6. Stability of non-Fermi-liquid State

In the above sections we have shown the NFL behavior of the system with the non-Kramers doublet CEF ground state. Because the low energy spectrum of the NFL part has the same form as that of $S=1/2$ -TCKM, an entropy at the zero temperature is expected to remain. However, it conflicts with the law of thermodynamics. The residual entropy should be released by some remaining mechanisms. We have shown when the magnetic field is applied, the NFL state breaks below the low energy, $H_z/10$, so the residual entropy is released.

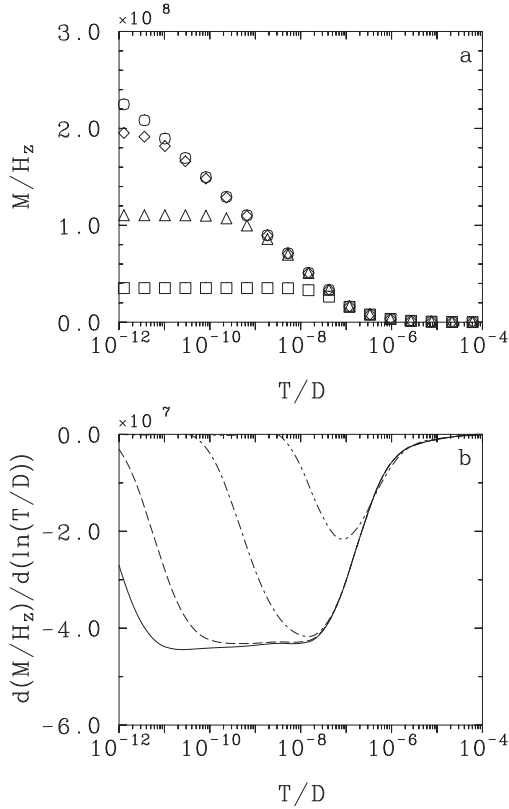


Fig. 12. Temperature dependence of the magnetizations (a) and the differential of them by the logarithm of temperature (b) under the orthorhombic CEF. The magnetic field $H_z = 1 \times 10^{-10}$ is applied. The split of the two singlets of f^2 configuration is; $\delta = 0$ (\circ , solid line), 2.2×10^{-9} (\diamond , dashed line), 2.1×10^{-8} (\triangle , dot-dashed line), 2.1×10^{-7} (\square , two-dots-dashed line), respectively. The occupation number of the f-electron for $\delta = 0$ is 1.91.

We study an effect of the lowering of the crystal symmetry as another possible mechanism. When the crystal symmetry changes from the tetragonal type to the orthorhombic one, the non-Kramers

doublet CEF ground state splits into two singlets. If the split is large enough, the low energy states is expected to follow the LFL model, and the entropy at low temperature will go to zero. In Fig. 12 (a) we show the normalized magnetizations for several cases of the orthorhombic CEF. When the split, δ , is zero, the result corresponds to that for the tetragonal CEF. Because the applied magnetic field, H_z , is very weak, the magnetization shows $-\ln T$ dependence for wide temperature region; from $T^* \sim 10^{-8}$ to $H_z/10 \sim 10^{-11}$. The $-\ln T$ dependence of the magnetic susceptibility is suppressed in the low temperature region, $T < \delta/10$. But for the small split, the $-\ln T$ dependence is still shown for the temperature region from T^* to $\delta/10$ as shown in Fig. 12 (b). The region is decreased with increasing δ , and it disappears for $\delta \sim T^*$. The saturation of the magnetization occurs in the temperature range where the energy spectrum is explained by the LFL Hamiltonian. The residual entropy will be released at the temperature that the magnetization saturates. If the lowering of the crystal symmetry is not large, the NFL behavior will be observed in a restricted temperature region.

§7. Summary

We have investigated the NFL state of the IAM with non-Kramers doublet ground state of the f^2 configuration under the tetragonal CEF. The low energy spectra, the temperature dependence of the magnetizations and the magneto resistances of the model are calculated by employing the NRG method. The spectra are explained by the combination of the NFL and the LFL parts which are independent with each other. One orbital of electrons with the $\Gamma_7^{(1)}$ symmetry contributes to the spectrum of LFL part, and the other two orbitals contribute to that of the NFL part. The phase shift of the conduction electron for the LFL component becomes very small at very low energy. The NFL part of the spectra has the same form to that of $S=1/2$ -TCKM which has been derived by the CFT.

The magnetization under the weak magnetic field shows the $-\ln T$ dependence, and it saturates below the temperature, $H_z/10$. The coefficient of the $-\ln T$ term has magnitude of $1/T^*$, where T^* is the temperature that the $-\ln T$ dependence begins. The saturation is consistent with the break of the NFL state under the magnetic field. The magnetization is well scaled by T^* and $M^* = M(T = T^*, H_z/T^* \ll 1)$. The magnetic field dependence of the phase shift is calculated from the low energy spectrum. When the hybridization is weak, the scattering amplitude decreases with increasing the magnetic field. But for large hybridization, the scattering amplitude increases. The existence of the positive magneto resistance suggests that the resistivity decreases with decreasing temperature. We have the parameter region for the IAM that the $-\ln T$ term of the magnetic susceptibility has the sizable coefficient, and the resistivity decreases with decreasing temperature. There is the possibility that the anomalous properties of $U_x\text{Th}_{1-x}\text{Ru}_2\text{Si}_2$ can be explained by the NFL scenario of the TCKM type for the present IAM. However, Actual U ion obeys L - S coupling scheme, so we need to consider complicated structures of the electronic states of the multi-electron

configurations for the quantitative discussions.

The lowering of the crystal symmetry breaks the NFL behavior at the temperature about $\delta/10$, where δ is the orthorhombic CEF splitting. The residual entropy is released at around this temperature. If δ is small, the NFL behavior is still expected in the intermediate temperature range.

Acknowledgments

We would like to thank H. Amitsuka, M. Koga, H. Shiba and Y. Kuramoto for useful discussions and comments. This work has been partly supported by Grant-in-Aid Nos. 06244104, 09640451 and 09244202 from the Ministry of Education, Science and Culture of Japan. The computation has been done at ‘the Computer Center, Tohoku University’, ‘the facilities of the Supercomputer Center, Institute for Solid State Physics, University of Tokyo’ and ‘the Computer Center of Institutes for Molecular Science, Okazaki National Research Institutes’.

-
- [1] H. Amitsuka, T. Hidano, T. Honma, H. Mitamura and T. Sakakibara: *Physica B* **186-188** (1993) 337.
 - [2] H. Amitsuka and T. Sakakibara: *J. Phys. Soc. Jpn.* **63** (1994) 736.
 - [3] H. Amitsuka, T. Sakakibara, A. de Visser, F. E. Kayzel and J. J. M. France: *Physica B* **230-232** (1997) 613.
 - [4] D. L. Cox: preprint, cond-mat/9704103, to be published in *Adv. Phys.*
 - [5] D. L. Cox: *Phys. Rev. Lett.* **59** (1987) 1240.
 - [6] D. L. Cox: *Physica B* **186-188** (1993) 312.
 - [7] P. Nozières and A. Blandin: *J. Phys. (Paris)* **41** (1980) 193.
 - [8] A. M. Tsvetick and P. B. Wiegmann: *J. Stat. Phys.* **38** (1985) 125.
 - [9] P. D. Sacramento and P. Schlottmann: *Phys. Rev. B* **43** (1990) 295.
 - [10] I. Affleck and A. W. W. Ludwig: *Phys. Rev. B* **48** (1993) 7297.
 - [11] O. Sakai, Y. Shimizu and N. Kaneko: *Physica B* **186-188** (1993) 322.
 - [12] H. Kusunose, K. Miyake, Y. Shimizu and O. Sakai: *Phys. Rev. Lett.* **76** (1996) 271.
 - [13] O. Sakai, S. Suzuki, Y. Shimizu, H. Kusunose and K. Miyake: *Solid State Commun.* **99** (1996) 461.
 - [14] S. Suzuki, O. Sakai and Y. Shimizu: *Solid State Commun.* **104** (1997) 429.
 - [15] M. Koga and H. Shiba: *J. Phys. Soc. Jpn.* **64** (1995) 4345.
 - [16] M. Koga and H. Shiba: *J. Phys. Soc. Jpn.* **65** (1996) 3007.
 - [17] M. Koga and H. Shiba: *J. Phys. Soc. Jpn.* **66** (1997) 1485.
 - [18] O. Sakai, S. Suzuki and Y. Shimizu: *Solid State Commun.* **101** (1997) 791.
 - [19] Y. Shimizu, O. Sakai and S. Suzuki: The analysis of the low energy spectrum will be partly published in *J. Mag. & Mag. Mat.*
 - [20] P. H. Butler: *Point Group Symmetry Applications, Methods and Tables* (Plenum Press, New York, 1981).
 - [21] H. R. Krishna-Murthy, J. W. Wilkins and K. G. Wilson: *Phys. Rev. B* **21** (1980) 1003.
 - [22] I. Affleck, A. W. W. Ludwig, H. B. Pang and D. L. Cox: *Phys. Rev. B* **45** (1992) 7918.
 - [23] The small difference may be due to the residual small interaction between the NFL and the LFL parts because we listed the energies at $L = 31$ step.
 - [24] H. Amitsuka: private communication.